Environ Earth Sci
DOI 10.1007/s12665-011-1097-6

ORIGINAL ARTICLE

Hydrochemistry of superficial waters in the Adoria mine area (Northern Portugal): environmental implications

Paulo J. C. Favas · João Pratas · M. Elisa P. Gomes

Received: 29 April 2010 / Accepted: 4 May 2011

Abstract The purpose of this work is to characterize the hydrochemical behavior of acid mine drainages (AMD) and superficial waters from the Adoria mine area (Northern Portugal). Samples of superficial and mine drainage water were collected for one year, bi-monthly, with pH, temperature, Eh, conductivity and HCO_3 determined in situ with chemical analyses of SO_4, Ca, K, Mg, Na, Cl, Ag, As, Bi, Co, Cu, Fe, Mn, Ni, Pb, Zn and Cd. In the mine, there are acidic waters, with low pH and significant concentrations of SO_4, and metals (Fe, Mn, Zn, Cu, Pb, Cd and Ni), while in the superficial natural stream waters outside the mine, the pH is close to neutral, with low conductivity and lower metal concentrations. The stream waters inside the mine influence are intermediate in composition between AMD and natural stream waters outside the mine influence. Principal Component Analysis (PCA) shows a clear separation between AMD galleries and AMD tailings, with tailings having a greater level of contamination.

P. J. C. Favas (✉) · M. E. P. Gomes
Department of Geology, School of Life Sciences and the Environment, University of Trás-os-Montes e Alto Douro, Apartado 1013, 5001-801 Vila Real, Portugal
e-mail: pjcf@utad.pt

J. Pratas
Department of Earth Sciences, Faculty of Sciences and Technology, University of Coimbra, Coimbra, Portugal

P. J. C. Favas · J. Pratas · M. E. P. Gomes
Geosciences Center, Faculty of Sciences and Technology, University of Coimbra, Coimbra, Portugal

Keywords Abandoned mine · Acid mine drainages · Water contamination · Heavy metals

Introduction

As a consequence of mining exploration for metallic mineral deposits, large quantities of sulfides are exposed to weathering processes (oxygen, water and bacteria) that generate acidic environments and promote the solubilization of the metal and/or semi-metal components of these minerals. Water acts as a reagent, as an environment where the reactions develop, and as a transport vector of the formed products making up the denominated acid mine drainage (AMD) (Schmiermund and Drozd 1997; Gomes and Favas 2006; Cánovas et al. 2007; Seal and Shanks 2008; Koski et al. 2008; Foster et al. 2008; Silva et al. 2009; Valente and Gomes 2009; Romero et al. 2010).

The impacts associated with AMD arise during mining work and progressively stress the environment after the abandonment of explorations. Without maintenance, the circulation of water inside the galleries and in the tailings occurs freely, causing effluents with high pollutant potential that easily migrate into various natural systems.

The main objective of this study was to better understand the hydrochemistry of superficial waters in the Adoria mine area (Northern Portugal). A summary of the geology and the mineralization typology of the Adoria mine area is presented. Results of water tests from mining galleries and tailings are compared with natural stream waters from inside and outside the mined area using data collected over a period of one year. Principal Component Analysis (PCA) is applied to statistically characterize the

Published online: 01 June 2011

data from this acidic water and superficial water drainage system.

Geographical and geological setting

The Adoria mine (or Cerva mine), which has several concessions, is situated in the parish of Cerva in the council of Ribeira de Pena district of Vila Real (Northern Portugal). Mineralized quartz veins cut medium- to coarse-grained two mica granites of porphyritic tendency, denominated Adoria mine granite and muscovitic aplogranite, which belong to the composite massif of Vila Real (Fig. 1). The veins fill subhorizontal fractures in the granites and the mines were originally explored for wolframite, cassiterite and polymetallic sulfides (Pereira 1989). The extractive activity occurred between the 1940s and 1980s, raising the number of tailings near the tributaries of the Poio River.

Although the Adoria mine granite is embedded quartz veins that shelter the Adoria mineralization, it does not look at all responsible for it. According to Pereira (1987, 1989), tin mineralization is found in a cupola of endogranite (aplogranite) with "stockscheider" associated. The levels obtained for Sn by Pereira (1987) show that both the granite from the Adoria mine and "stockscheider" can be considered Sn-bearing granites (Lehmann 1990). The W levels are relatively low in the two granite groups and in the "stockscheider"; however, they are slightly higher in the Adoria mine granite.

According to the designation used by authors cited by Arribas et al. (1981), such as Baumann (1970), Charoy (1975) and Nesen (1981), it seems we are in the presence of a mineral deposit that follows the exogranite–endogranite with "stockscheider" organization model.

According to Pereira (1987), the mineralization of the Adoria mine occurs in quartz veins of two generations:

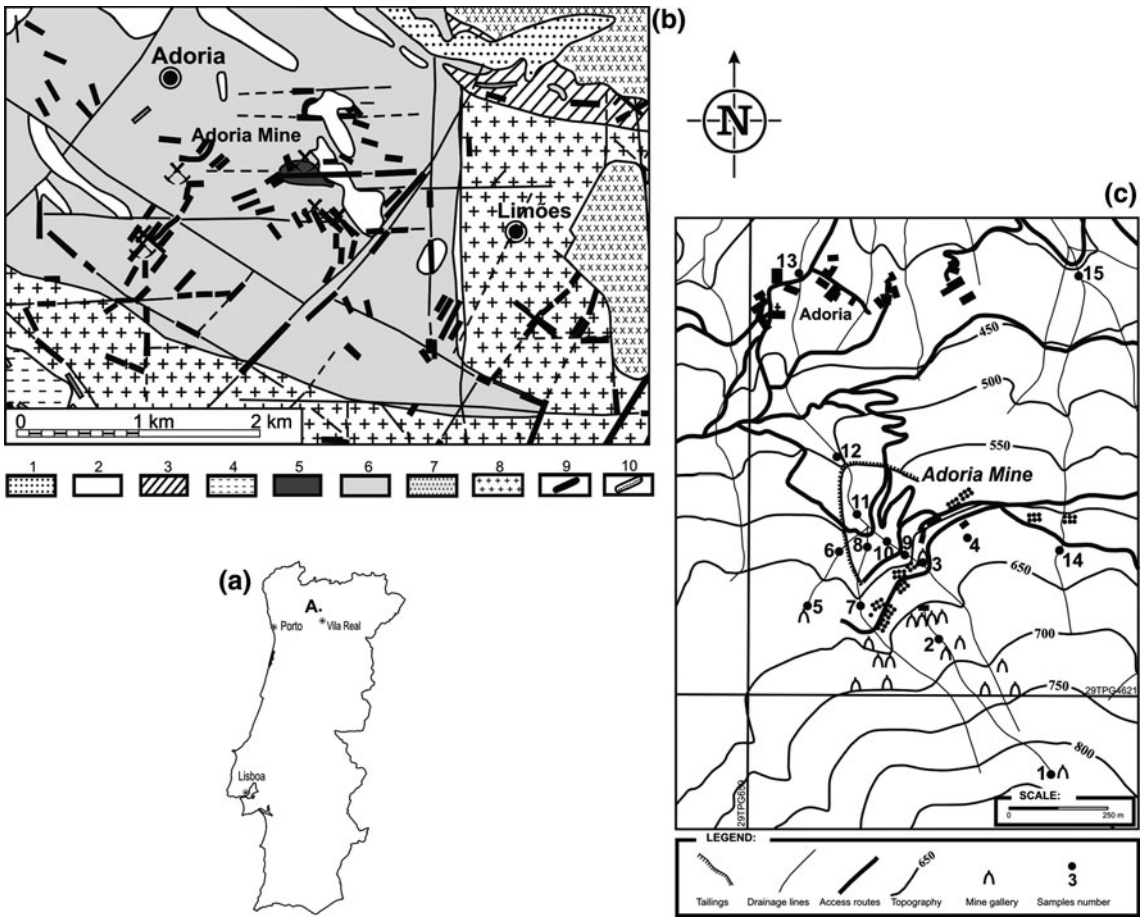

Fig. 1 **a** Location of the abandoned Adoria mine on the map of Portugal; **b** simplified geological map of Adoria area (adapted from the Portugal Geological Map, 10-A, Celorico de Basto); *1* alluvium, *2* "Santos Formation" (Silurian/Devonian metasedimentary rocks: metapelite, metasiltstone, metagreywacke), *3* pelitic and carbonaceous hornfels, *4* "Vila Nune Unit" (Silurian/Devonian metasedimentary rocks: quartzite, metavulcanite, schist, *5* moscovitic aplogranite, *6* Adoria mine granite, *7* fine-grained two mica granite, *8* Vila Real granite, *9* quartz veins, *10* pegmatite veins; **c** simplified topographical map with water sampling points

poor sub-vertical ones filling traction cracks generated by the combined shear ductile-fragile N–S and W–E system, which are right handed and sinistral, respectively; and other richer and more powerful sub-horizontal veins cuts the previously mentioned sub-vertical veins and corresponds to the filling of traction cracks depending on the cooling of the granite massif and the mineralizing fluid tension linked to the final granite crystallization.

Methodology

Sampling and samples preparation

Fieldwork included the identification and sampling of the different acid mine effluents and stream waters, as well as samples of ore minerals from the tailings, mine galleries and outcrops of the mine. For the characterization of the mine effluents (AMD), samples from the drainage galleries and tailings were collected. To evaluate the impact of the AMD in the fluvial system reference points were established at the confluences with mine effluents or with the receiving water lines. Downstream of those confluences, sampling was conducted toward the longitudinal space in order to examine the self-purification characteristics of the receiving environment. The field area and the location of water samples are shown in Fig. 1c.

The defined sample stations were sampled for a year between January and November of 2003 in six bi-monthly sampling campaigns. Samples were collected in polyethylene containers, washed with distilled water dipped underwater for at least 24 h in 10% HNO_3 and then rinsed with distilled water. Immediately after collection, all samples were placed in thermal freezers where the temperature was kept at approximately 4°C (ASTM 2011; USEPA 1991).

Portable instruments were used to measure pH, Eh, temperature and electric conductivity (EC). The HCO_3 is also measured in situ by titration.

Analytical methods

The ore minerals were analyzed using a Cameca Camebax electron-microprobe and a Jeol JXA-8500F at the National Laboratory of Energy and Geology (LNEG) (Porto, Portugal). Analyses were conducted using an accelerating voltage of 15 kV and a beam current of 20 and 10 nA in the Cameca and the Jeol microprobes, respectively. Standards included cassiterite (Sn-Lα), $MnTiO_3$ (Mn-Kα and Ti-Kα), Fe_2O_3 (Fe-Kα), sphalerite (Zn-Kα and S-Kα), pyrite (Fe-Kα and S-Kα), galena (Pb-Mα), arsenopyrite (As-Lα), Cr_2O_3 (Cr-Lα), Ta (Ta-Mα), Nb (Nb-Lα), W (W-Lα), Cd (Cd-Lα), Bi (Bi-Mα), Sb (Sb-Lα), Cu (Cu-Kα), Ni (Ni-Kα), Mo (Mo-Lα) and Ag (Ag-Lα).

The water was filtered and acidified for determination of As and metals. Laboratory analyses were performed at the Chemical Laboratory of the Department of Earth Sciences, University of Coimbra (Portugal) using current analytical methods [Atomic Absorption Spectrometry (AAS) for Ca, Mg, Na and K; coupled graphite furnace AAS for Fe, Mn, Cu, Zn, Cd, Co, Ni, Pb and As; the spectrophotometric method for Cl; SO_4 was analyzed by gravimetry]. Water data quality control was performed by inserting reagent blanks and duplicate samples into each batch. Analytical precision, defined as the percent relative variation at the 95% confidence level, ranged from 2–6%, depending on the concentration levels. The detection limits for major and trace elements in water samples were 0.025 mg/L SO_4, Cl; 0.5 mg/L Ca; 0.1 mg/L Mg; 1 mg/L Na, K; 10 μg/L Fe; 2.5 μg/L Mn; 6 μg/L Zn; 0.1 μg/L Cu, Pb; 0.5 μg/L As; 0.05 μg/L Cd; 0.02 μg/L Co; and 5 μg/L Ni.

Statistical testing

To facilitate and improve the interpretation of hydrogeochemical data, we applied principal components analysis (PCA). The data matrix used in the analysis consisted of 60 samples and 17 variables (pH, HCO_3, SO_4, Ca, Mg, Na, K, Cl, Fe, Mn, Zn, Cu, Pb, As, Cd, Co and Ni).

Results and discussion

Mineralization typology

Wolframite is the main W ore of the Adoria mine and is associated with cassiterite and scheelite as well as several sulfides of iron, copper, lead and zinc. The principal gangue minerals associated with the Adoria mineralization include quartz and some muscovite.

Studies on the mineralogy and geochemistry of the Adoria mine veins (Fig. 2; Table 1) show that wolframite occurs in large quantities in prismatic, euhedral or subhedral crystals, sometimes fractured and conjoined by quartz (Fig. 2b). Pyrite is a dominant sulfide and is one of the first to crystallize from solution (Fig. 2c, d). It shows up in both crystals and masses and is generally idiomorphic. It presents sphalerite inclusions and fractures filled by galena. Sphalerite is one of the first sulfides to deposit. It frequently has chalcopyrite exsolutions ("chalcopyrite disease") and occurs as an inclusion in galena. The late generation of sphalerite shows more chalcopyrite exsolutions and pyrrhotite inclusions. Stannite can fill fractures in sphalerite (Fig. 2f), and sphalerite can also occur as exsolution in pyrite. Chalcopyrite is anhedral and occurs in masses

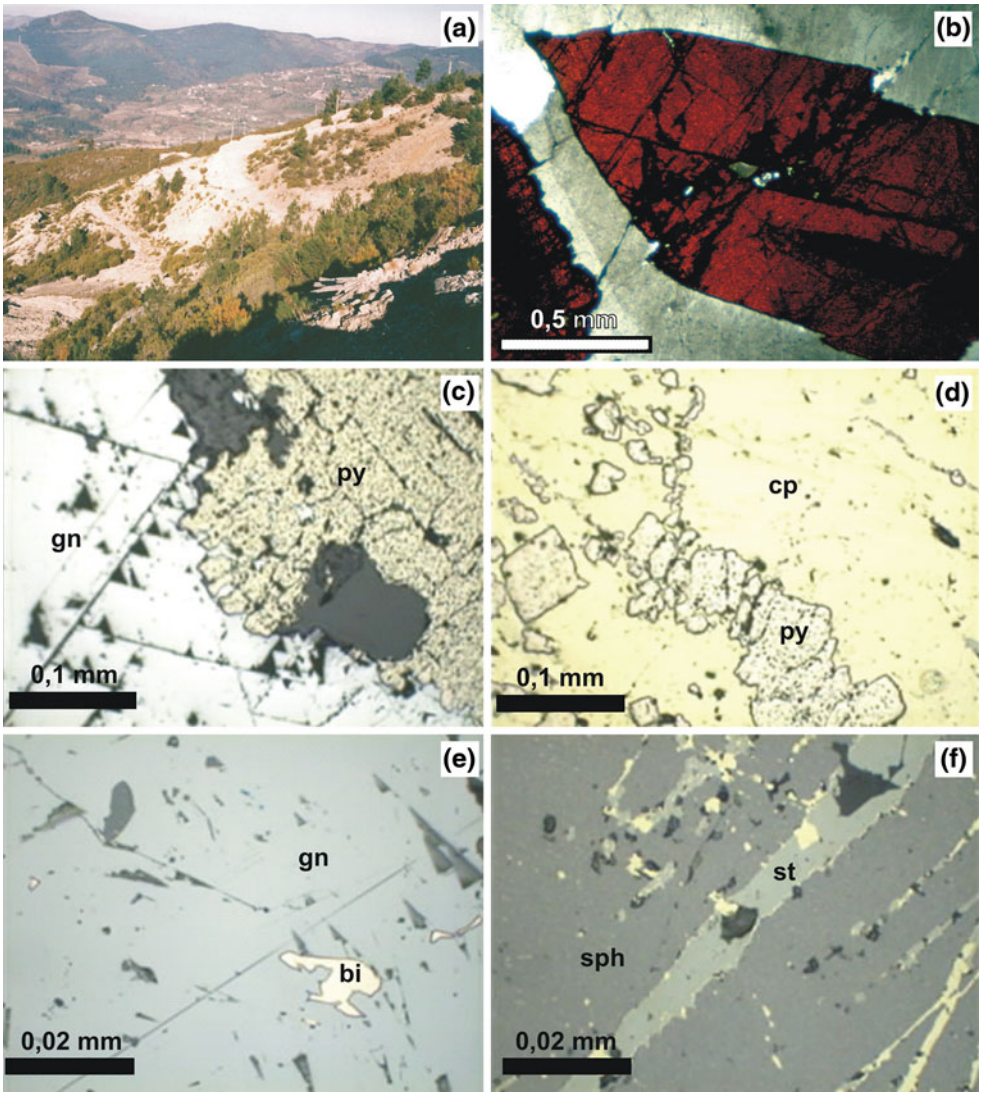

Fig. 2 **a** Adoria mine tailings; **b** Wolframite crystal (*natural light*, *PN*); **c** galena (*gn*) and pyrite (*py*) (*reflected light*); **d** pyrite inclusions in chalcopyrite (*cp*) (*reflected light*); **e** galena with bismuth inclusion (*bi*) (*reflected light*); **f** sphalerite (*sph*) cut by veinlets of stannite (*st*) (*reflected light*)

conjoining earlier minerals in both sphalerite inclusions and in galena or filling fissures in several minerals. Sphalerite and pyrite inclusions also occur in chalcopyrite (Fig. 2d). Pyrrhotite is quite commonly observed as relics included in sphalerite and galena. Stannite is generally xenomorphic and occurs as inclusions in chalcopyrite and along the sphalerite fissures. Galena occurs in anhedral crystals, normally taking up other mineral's fissures (sphalerite) or absorbing them (pyrite and chalcopyrite) (Fig. 2c). It seems to have been one of the last sulfides to form. It shows several native bismuth inclusions (Fig. 2e), pyrrhotite, chalcopyrite and sphalerite. Cassiterite and scheelite are also referred by Pereira (1987) as a component of the Adoria mineralization subordinated to wolframite.

Geochemistry of waters

The results of chemical analysis of the water samples are given in Table 2. The results verify that waters from the galleries and from the tailings generally present the chemical characteristics of the sulfide leaching process, exhibiting pH values between 4.18 and 7.49, an elevated metallic charge and the dominant anion of sulfate. Piper's triangular diagrams classify these waters as dominantly mixed sulfated and sodic sulfated throughout the whole sampling year.

The stream-water samples in the surrounding mines generally have low ionic charge with EC varying between 13.7 and 78.0 µS/cm. In this group, it is possible to distinguish the samples from the stream water outside the

Table 1 Representative chemical analyses of sulphides from the Adoria mine

	Galena ($n = 62$)	Pyrite ($n = 55$)	Sphalerite ($n = 23$)	Chalcopyrite ($n = 19$)	Stannite ($n = 7$)	Pyrrhotite ($n = 8$)
Fe	0.15	46.70	8.88	29.79	11.22	58.67
Mn	0.03	0.02	0.30	0.01	0.01	0.01
Cu	0.08	0.15	0.77	35.17	29.30	0.08
Zn	0.10	0.08	57.09	0.51	2.71	0.04
Pb	84.21	0.19	0.02	0.10	–	0.18
Cd	–	0.04	0.71	0.04	0.14	0.09
Bi	0.92	–	–	–	–	–
Sn	–	0.09	–	–	27.82	–
Ag	1.49	0.03	0.04	0.03	0.003	0.03
As	0.03	0.07	0.03	0.07	0.004	0.08
Sb	0.03	0.03	0.03	0.03	0.02	0.05
S	13.79	53.93	33.38	34.79	29.50	39.94
Total	99.98	100.93	101.20	100.33	100.71	99.08

mine area, which present pH values close to neutral, from the stream-water samples inside the mine influence, which present pH values in the weak acid range and have significant Mn and SO_4 levels. Piper's triangular diagrams classify these waters as dominantly mixed sulfated or sodic sulfated, while the local hydrochemical background waters are classified as dominantly chlorinated and sodic sulfated.

Using the classifications of Ficklin et al. (1992) for mine waters and mineralized areas (these are based on the variations of the levels of Zn, Cu, Cd, Ni, Co, and Pb in the solution as a function of pH), it is possible to determine the waters' typology at the different sampling stations (Fig. 3). According to this classification, every sample of the stream-waters outside the mine influence presents low metal content in solution, varying between "acid" and "near-neutral". The AMD samples are divided into two groups with different typologies. One group has elevated heavy metal contents ("high metals") and low pH values ("acid"), and the other has "low metal" waters with pH values between "acid" and "near-neutral". The first group is water from the surface and from the base of the tailings, while the second group is the collected drainage from the mine galleries. The stream-water samples inside the mine influence appear identical to those of the AMD and are classified as "acid" and "high metal". The stream-water samples are under direct influence of the runoff of the tailings.

The results clearly show the sulfated character of the studied water, particularly the AMD samples, and the stream-waters inside the mine influence. These are characterized by important sulfate addition even when significant increases in the conductivity and metal values and declining pH values are not verified (Fig. 4).

Acid mine drainage is controlled by the leaching process of mineralized veins with sulfides. The hydrochemical features in the Adoria area appear to be dominated by the oxidation of Fe-bearing sulfide minerals (pyrite, chalcopyrite, pyrrhotite, galena and sphalerite) producing H^+, SO_4^{2-} and metals (Me) in solution (aq), as in the following reactions proposed by Cidu et al. (1997):

$$(\mathrm{Fe},\ \mathrm{Me})\mathrm{S}_2 + 3.5\mathrm{O}_2 + \mathrm{H}_2\mathrm{O} \rightarrow \mathrm{Fe}_{\mathrm{aq}}^{2+},\ \mathrm{Me}_{\mathrm{aq}}^{2+} + 2\mathrm{SO}_4^{2-} + 2\mathrm{H}^+$$

$$2\mathrm{Fe}_{\mathrm{aq}}^{2+} + 0.5\mathrm{O}_2 + 2\mathrm{H}^+ \rightarrow 2\mathrm{Fe}_{\mathrm{aq}}^{3+} + \mathrm{H}_2\mathrm{O}$$

The AMD composition of the Adoria mine and evolving superficial waters clearly reflect the seasonal flotation influence even as important variations are registered in the majority of the analyzed parameters. In the dry season, lower pH levels are observed, and the conductivity and metal concentration levels are higher. The data collected verify, in general terms, that water quality (Portuguese law, 2007, Decree no. 306/2007) varies with the seasonal regime, with contamination levels more significant in dry periods than in humid periods.

The application of PCA to the hydrochemical data resulting from the six sampling campaigns at the Adoria mine focused on the matrix of 60 individuals (samples) and 17 variables (pH, HCO_3, SO_4, Ca, Mg, Na, K, Cl, Fe, Mn, Zn, Cu, Pb, As, Cd, Co and Ni). Our results show that five principal factorial axes explain more that 80% of the total variance, as shown in Fig. 5. Only Fe does not appear to be well explained in the first five axes, presenting higher correlation in the sixth axis.

Thus, considering the six retained axes and attending to the coordinate values, the following affiliations are

Table 2 Chemical compositions of AMD and stream waters inside and outside mine influence, from the Adoria abandoned mine

Sample	Type	Field parameters			Major anions (mg/L)		Major cations (mg/L)				Trace elements (μg/L)								
		pH	EC (μS/cm)	HCO_3 (mg/L)	SO_4	Cl	Ca	Mg	Na	K	Fe	Mn	Zn	Cu	Pb	As	Cd	Co	Ni
1 Jan	AMD	7.49	15.20	5.61	21.48	1.92	0.45	0.15	1.86	0.34	505.00	58.00	100.00	5.00	3.00	0.52	1.20	0.48	11.89
2 Jan	IMI	7.41	13.70	5.13	27.24	1.84	0.30	0.13	1.79	0.35	114.00	10.00	105.00	6.00	4.00	0.98	1.26	0.12	40.88
3 Jan	AMD	5.62	20.20	7.49	15.71	1.85	1.06	0.53	1.80	0.36	41.00	37.00	156.00	46.00	15.00	1.93	1.87	0.52	17.79
4 Jan	IMI	5.44	17.30	5.23	6.81	1.69	0.50	0.20	1.64	0.28	67.00	29.00	158.00	26.00	9.00	1.80	1.90	0.24	13.84
5 Jan	AMD	5.18	21.80	6.54	18.33	2.20	0.50	0.24	2.13	0.40	27.00	26.00	113.00	7.00	3.00	0.80	1.36	0.44	11.00
6 Jan	IMI	7.50	16.50	5.51	11.41	1.95	0.32	0.21	1.89	0.33	62.00	4.00	132.00	7.00	5.00	0.55	5.28	0.31	24.39
7 Jan	IMI	4.43	41.80	5.95	262.37	1.60	0.78	0.24	1.55	0.41	304.00	2.00	492.00	357.00	32.00	1.45	24.60	0.73	27.69
8 Jan	AMD	4.38	56.40	11.11	277.45	2.35	2.21	0.61	2.28	0.46	84.00	39.00	718.00	273.00	187.00	1.70	28.72	0.82	26.37
9 Jan	AMD	5.32	21.90	6.98	34.04	1.87	1.10	0.23	1.81	0.35	35.00	27.00	238.00	56.00	23.00	1.20	5.95	0.48	16.47
10 Jan	AMD	4.68	51.60	12.47	16.40	2.33	2.76	0.81	2.26	0.40	77.00	15.00	792.00	177.00	82.00	1.09	0.95	1.72	23.07
11 Jan	AMD	4.54	52.60	9.97	28.70	2.11	2.00	0.54	2.05	0.40	27.00	60.00	640.00	264.00	159.00	2.27	8.96	1.48	15.81
12 Jan	IMI	4.50	52.70	9.92	24.60	2.07	1.97	0.55	2.01	0.43	78.00	15.00	735.00	261.00	170.00	1.61	0.88	1.32	18.45
13 Jan	IMI	4.69	54.80	12.99	15.32	2.73	2.48	0.61	2.65	0.75	68.00	15.00	632.00	197.00	108.00	1.25	8.85	1.45	41.54
14 Jan	OMI	4.61	18.40	4.62	8.04	1.67	0.25	0.14	1.63	0.30	46.00	38.00	190.00	17.00	6.00	0.66	2.28	0.71	18.05
15 Jan	OMI	7.10	25.00	8.46	7.04	2.61	0.88	0.30	2.54	0.52	224.00	2.00	195.00	30.00	5.00	0.57	0.23	1.12	13.95
1 Mar	AMD	6.05	17.20	6.19	26.19	3.51	0.52	0.17	2.06	0.34	13.00	18.00	178.00	12.00	6.00	1.32	2.14	0.42	7.00
2 Mar	IMI	6.20	15.40	5.72	35.00	3.39	0.42	0.13	1.99	0.32	43.00	60.00	175.00	4.00	4.00	1.86	2.18	0.19	8.00
3 Mar	AMD	5.99	22.20	7.31	16.76	3.31	1.12	0.28	1.95	0.31	102.00	16.00	214.00	74.00	19.00	1.59	2.57	0.48	7.35
4 Mar	IMI	5.57	19.10	5.69	5.45	2.88	0.62	0.23	1.69	0.30	14.00	32.00	250.00	47.00	13.00	1.84	3.00	0.28	6.94
5 Mar	AMD	5.10	23.20	6.98	26.19	4.01	0.47	0.26	2.36	0.41	13.00	17.00	193.00	3.00	5.00	1.16	2.32	0.55	8.10
7 Mar	IMI	4.73	34.80	10.71	296.09	2.57	3.25	0.25	1.51	0.35	299.00	87.00	525.00	351.00	33.00	2.00	26.25	0.78	7.18
8 Mar	AMD	4.63	42.10	8.41	188.54	3.05	1.69	0.31	1.80	0.41	430.00	11.00	531.00	307.00	173.00	1.30	21.24	0.96	7.35
9 Mar	AMD	5.49	24.90	7.52	29.96	3.25	1.41	0.27	1.91	0.18	270.00	23.00	301.00	43.00	13.00	3.42	7.53	0.86	9.10
10 Mar	AMD	4.36	77.10	17.18	13.94	4.59	4.27	1.23	2.70	0.39	28.00	9.00	1,350.00	247.00	169.00	1.91	1.62	2.46	8.92
11 Mar	AMD	4.44	74.60	15.70	40.22	4.38	3.82	1.06	2.58	0.39	352.00	27.00	1,176.00	271.00	156.00	2.11	16.46	1.42	9.20
12 Mar	IMI	4.28	67.60	13.44	23.78	4.27	2.94	0.83	2.51	0.43	35.00	18.00	970.00	276.00	201.00	2.09	1.16	1.15	9.32
13 Mar	IMI	4.75	64.80	15.95	16.00	5.28	3.23	0.86	3.11	0.78	35.00	5.00	750.00	219.00	119.00	1.41	10.50	1.19	9.07
15 Mar	OMI	5.54	27.80	23.69	6.53	4.61	8.04	0.59	2.71	0.51	249.60	40.00	99.00	63.00	15.00	1.36	0.12	1.09	9.28
1 May	AMD	6.05	17.70	7.48	18.50	4.79	0.59	0.04	2.82	0.29	12.45	47.00	98.32	30.90	1.56	0.69	2.04	0.27	14.69
2 May	IMI	6.17	17.70	7.48	21.50	3.50	1.06	0.06	2.06	0.56	130.53	8.10	103.24	28.40	55.04	1.30	2.11	0.34	50.51
3 May	AMD	5.44	26.60	6.85	14.14	3.32	1.03	0.17	1.95	0.28	33.64	29.98	135.84	44.10	16.01	2.57	1.63	0.24	21.99
11 May	AMD	4.42	67.10	13.70	20.50	5.05	2.61	0.85	2.97	0.41	16.85	260.18	694.86	234.60	203.67	1.43	9.73	1.35	18.15

Table 2 continued

Sample	Type	Field parameters			Major anions (mg/L)		Major cations (mg/L)				Trace elements (μg/L)								
		pH	EC (μS/cm)	HCO_3 (mg/L)	SO_4	Cl	Ca	Mg	Na	K	Fe	Mn	Zn	Cu	Pb	As	Cd	Co	Ni
12 May	IMI	4.37	64.30	13.09	21.73	5.15	2.34	0.76	3.03	0.41	19.43	29.20	1132.84	208.10	193.86	1.02	1.36	1.01	39.36
15 May	OMI	5.56	28.20	8.40	6.03	4.80	0.82	0.12	2.82	0.43	140.56	1.82	166.06	17.70	0.18	0.27	0.20	0.97	2.76
1 Jul	AMD	6.48	18.80	5.72	22.40	3.79	0.36	0.03	2.23	0.24	32.84	94.00	100.41	27.40	2.36	0.76	2.24	0.48	15.54
2 Jul	IMI	6.70	18.40	3.28	40.78	2.24	0.17	0.02	1.32	0.13	14.38	16.21	105.43	32.40	60.09	1.41	2.28	0.26	53.43
3 Jul	AMD	5.44	34.10	6.33	10.48	3.13	0.92	0.15	1.84	0.26	80.48	59.97	156.64	34.90	20.69	2.79	1.88	0.38	23.26
11 Jul	AMD	4.38	79.00	13.70	68.90	5.31	2.34	0.74	3.13	0.65	29.68	179.73	642.61	195.50	212.61	3.28	20.00	1.14	2.60
12 Jul	IMI	4.44	69.80	14.15	21.16	5.73	2.55	0.72	3.37	0.44	52.39	32.29	623.06	164.40	201.68	2.33	0.75	0.59	3.04
15 Jul	OMI	5.47	36.50	6.31	5.03	3.60	0.62	0.12	2.12	0.31	75.13	2.81	44.91	5.50	6.59	0.82	0.05	0.66	2.83
1 Sep	AMD	6.00	28.00	5.30	29.50	3.59	0.34	0.02	2.11	0.18	20.94	180.00	126.79	4.01	4.50	1.04	2.89	0.45	17.49
2 Sep	IMI	5.22	22.00	3.10	63.22	2.09	0.14	0.03	1.23	0.15	69.26	31.03	133.13	4.81	84.00	1.94	3.00	0.12	60.15
3 Sep	AMD	5.12	38.00	6.02	16.24	2.98	0.94	0.10	1.75	0.22	164.30	114.83	197.79	36.90	22.50	3.83	2.37	0.50	26.18
11 Sep	AMD	4.18	89.00	13.10	88.50	4.90	2.24	0.69	2.88	0.74	416.53	452.67	811.45	465.02	1,021.58	4.51	35.00	2.14	41.03
12 Sep	IMI	4.23	78.00	13.84	22.00	5.61	2.46	0.67	3.30	0.49	59.50	35.29	931.90	459.74	1,092.25	1.59	1.12	1.91	47.87
15 Sep	OMI	5.22	35.00	6.02	8.04	3.50	0.58	0.10	2.06	0.27	200.00	2.91	249.85	30.00	7.78	0.67	0.30	1.71	20.45
1 Nov	AMD	6.10	18.00	6.34	16.20	2.35	0.48	0.10	2.28	0.31	24.24	88.16	77.46	7.80	3.26	1.04	2.00	0.23	10.58
2 Nov	IMI	5.34	18.30	5.44	18.95	1.87	0.45	0.11	1.82	0.34	80.19	15.20	81.33	9.35	4.35	1.94	2.10	0.06	36.38
3 Nov	AMD	5.20	19.80	7.02	22.00	2.02	1.08	0.18	1.96	0.29	190.22	56.24	178.92	71.72	16.31	4.10	2.15	1.18	15.84
4 Nov	IMI	5.28	14.60	5.38	7.66	1.63	0.60	0.20	1.58	0.31	37.52	44.08	122.39	18.64	9.79	4.38	1.47	0.12	12.31
5 Nov	AMD	5.16	22.00	6.30	25.46	2.16	0.45	0.22	2.10	0.38	34.84	39.52	87.53	5.02	3.26	1.58	2.00	0.21	9.79
7 Nov	IMI	4.78	36.00	9.20	112.90	1.46	2.66	0.20	1.42	0.32	113.68	1.66	179.28	302.54	27.31	0.51	8.96	0.48	17.37
8 Nov	AMD	4.71	33.10	8.76	96.97	1.82	1.84	0.32	1.77	0.45	44.87	3.41	519.62	162.69	21.19	0.52	20.78	0.49	9.89
9 Nov	AMD	5.40	17.50	7.50	24.00	1.87	1.36	0.30	1.82	0.27	32.67	22.34	167.26	22.33	13.46	0.52	4.18	0.15	10.99
10 Nov	AMD	4.59	43.50	16.90	12.30	2.73	4.50	0.88	2.65	0.42	101.38	22.80	1,039.38	108.84	61.50	1.23	1.25	1.78	12.16
11 Nov	AMD	4.46	49.70	15.60	21.36	2.83	3.64	0.96	2.75	0.45	35.55	23.77	625.65	215.21	160.59	2.87	8.76	1.32	15.38
12 Nov	IMI	4.37	53.70	13.68	18.86	2.78	2.88	0.84	2.70	0.42	142.35	22.80	1,101.83	205.40	171.70	1.06	1.32	1.20	15.56
13 Nov	IMI	4.55	52.10	15.10	11.57	3.01	3.15	0.80	2.92	0.68	43.07	40.38	607.54	203.25	72.36	0.82	8.51	0.07	25.61
14 Nov	OMI	5.04	17.80	5.72	5.53	1.93	0.32	0.33	1.87	0.34	40.79	76.00	179.65	8.84	4.90	0.44	2.16	0.36	17.49
15 Nov	OMI	5.67	27.00	17.88	6.78	2.76	5.54	0.25	2.68	0.47	145.85	0.67	171.10	12.90	5.38	0.27	0.21	1.18	3.25

AMD acid mine drainage, *IMI* inside mine influence, *OMI* outside mine influence

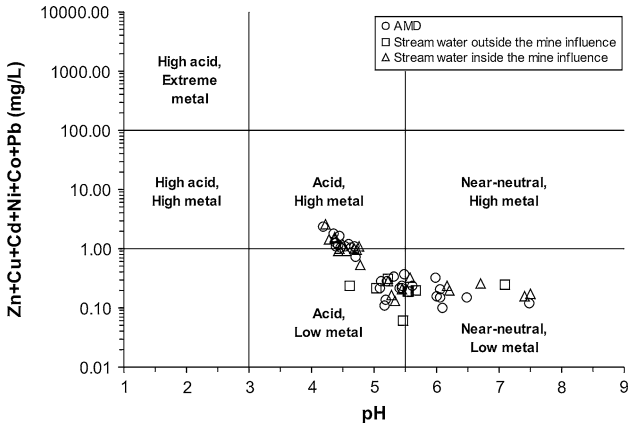

Fig. 3 Water samples from Adoria mine area plotted on the Ficklin et al. (1992) diagram based on pH and metal concentrations (Zn + Cu + Cd + Ni + Co + Pb)

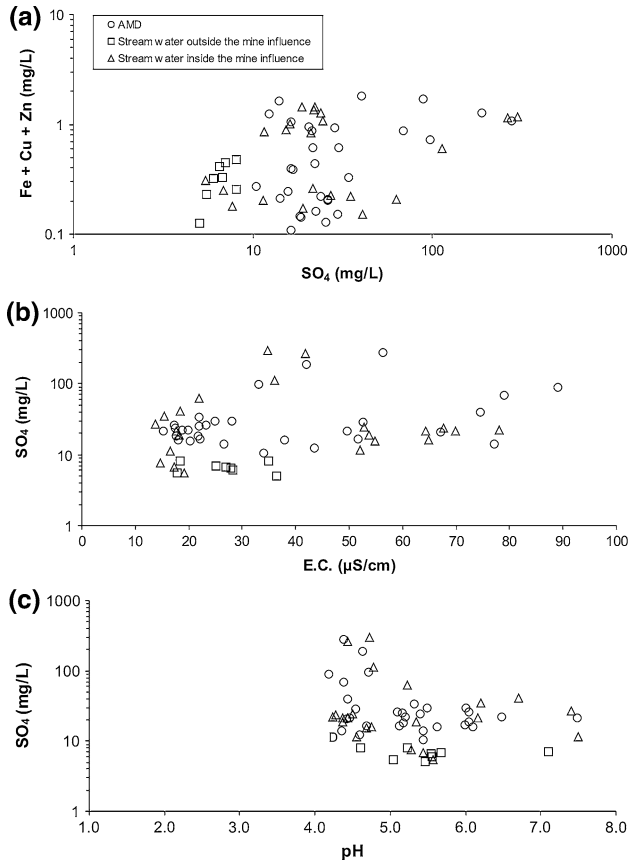

Fig. 4 **a** (Fe + Cu + Zn) versus SO_4 diagram; **b** SO_4 versus electrical conductivity (EC) diagram; **c** SO_4 versus pH diagram, for AMD, and stream waters inside the mine influence and outside the mine influence

verified: the first axis explains variables Mg, Zn, HCO_3, Cu, Co, Na, K, Ca, Pb and Cl in opposition to the pH variable, and the second axis explains variables SO_4, Cd and, in an unclear way, Fe. In particular, the Mn, Ni, As and Fe variables are explained by axes 3, 4, 5 and 6, respectively. Naturally, the first two axes are the most important because they explain a greater number of variables; they group variables and explain, as a whole, more that 58% of the total variance.

The combined analysis of the data and the interpretation of the variables verify, in the first factorial plan (Fig. 5), the existence of a variable association that indicates the influence of the geological context, which we split into three distinct groups: the first group is made up of HCO_3, Ca, K, Cl, Na, Mg, Zn and Co (axis 1); the second group is composed of SO_4 and Cd (and, in some way, Fe) (axis 2), which reveals an independent behavior to that of the first group; and the third group is intermediate between the previous two but with greater compatibility with the first, demonstrating a Cu and Pb association.

In the first and the second factorial plans (Fig. 5), there is a strong negative correlation between the Pb variable and the first group of variables. The SO_4 and the Cd (and Fe) seem to be independent of the pH.

The Ni, As and Mn variables are not considered in the analysis of the first factorial plan because its correlation coefficient with the plan is less than 0.5. In fact, Mn is explained by the third axis in the second factorial plan by its affinity to Pb and Cl. Ni is only explained by the fourth axis in the third factorial plan (Fig. 5) and is thus independent of pH and the variables HCO_3, Ca, K, Cl, Na, Mg, Zn, Co, Cu and Pb. Arsenic is explained by the fifth axis in the fourth factorial plan (Fig. 5) and reveals weak dependency on pH and the other variables. Fe is inadequately explained in the first factorial plan, improving only in the sixth axis in the fifth factorial plan, where it is isolated from the other variables.

Thus, the hydrochemistry of the area surrounding the Adoria mine is complex and difficult to interpret, especially beyond the first factorial plan. The first factorial axis seems to demonstrate that the study area is mainly influenced by mineralization and gangue signatures. This interpretation is reinforced by the variables' projections into the second, third and fourth factorial plans, which reveal the group's proximity to Cu and Pb variables from the HCO_3, Ca, K, Cl, Na, Mg, Zn and Co variables.

The samples' projection in the first factorial plan verifies the clear separation into three differentiated "populations" (Fig. 6). "Population" A is essentially made up of samples belonging to the local hydrochemical background; the AMD samples collected in the mine galleries, characterized by reduced metallic charge; and the samples inside the mine influence with a reduced pollutant charge. "Population" B results from the association of the most contaminated samples, the AMD samples generated in the tailings and the samples under direct influence of these runoff

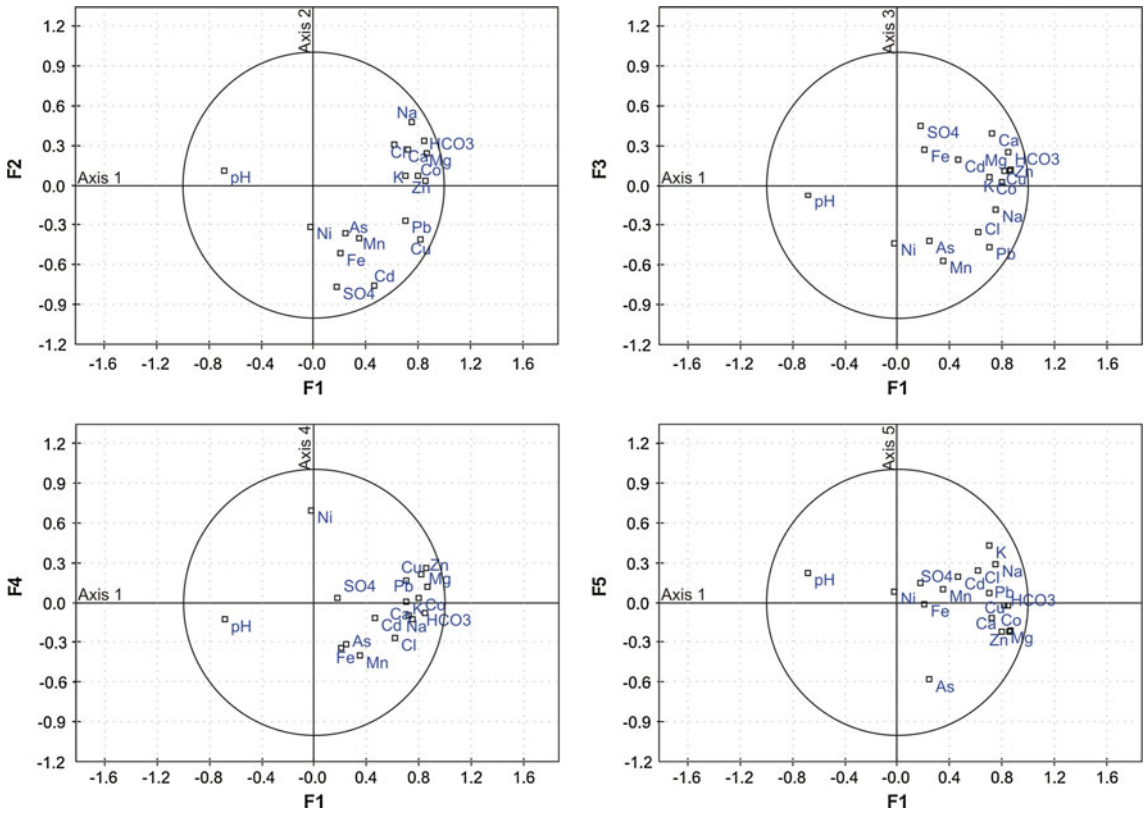

Fig. 5 Projection of the variables in the forth first factorial plans of the PCA

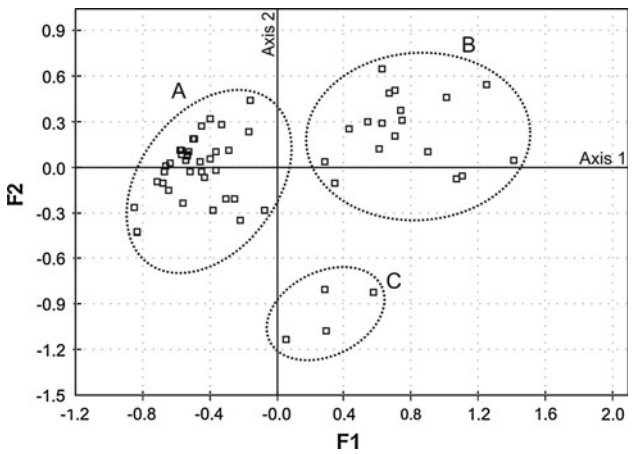

Fig. 6 Projection of the samples in the first factorial plan of the PCA

waters. This population is located in the HCO_3, Ca, K, Cl, Na, Mg, Zn and Co association influence area, and to some extent, Cu and Pb reflect the importance of the oxidation of the sulfides present in the tailings and the hydrolysis of silicates, the most abundant component deposited in the tailings. "Population" C is made up of samples from stations 7 and 8 that were sampled in January and March are under the influence of SO_4 and Cd, and could be related to the existence of numerous upstream mine galleries.

Conclusion

The AMD from the galleries and, above all, from the tailings present chemical characteristics that reflect the leaching process of mineralized masses with sulfides. Thus, these waters are characterized by having low pH values and high levels of sulfate and metals in solution.

The majority of superficial waters that circulate in upstream areas of mines are characterized by pH values close to neutral, conductivity that varies between 17.8 and 36.5 µS/cm and a low ionic charge. Sampled waters downstream from galleries and tailings reveal a withdrawal from these characteristics and an approximation to those evidenced by AMD.

Meanwhile, the environmental impact on the quality of the superficial waters is, above all, experienced in the closest surroundings of the pollution source (1–2 km). Several processes contribute to this situation: (1) dilution by other waters, groundwater and surface, that flow toward stream waters; (2) precipitation or co-precipitation of metallic cations in hydroxides and sulfates, allowing pH to rise; and (3) adsorption of the metallic cations by organic and inorganic sediments and aquatic plants.

The use of PCA, with the purpose of characterizing acidic drainage of the Adoria mine and the superficial waters surrounding it, allowed a clear separation of AMD

galleries and tailings; tailings had a greater level of contamination, as did the waters under direct influence, with an ionic charge characterized by HCO_3, Ca, K, Cl, Na, Mg, Zn, Co, and Cu and Pb association. An abundance of sulfide masses in the tailings explains this mixed typology and reveals influences by both silicate hydrolysis and oxidation of the sulfides.

Based on our research here, we advise additional studies to monitor the fluvial system surrounding the mine in order to follow and control the behavior of the most deleterious characters and to plan sampling campaigns of groundwater in the area surrounding this mine.

Acknowledgments The authors gratefully acknowledge the instrumental support of the Geosciences Centre at Coimbra University and financial support from FCT (Portuguese Foundation for Science and Technology) presented as a PhD Fellowship to P.J.C. Favas.

References

Arribas A, Gagny C, Hermosa J, Nesen G, Ovejero G, Servajean G (1981) Potencialidad metalogenica de las unidades exoendograniticas en el yacimiento Sn-W de Fontao (Galicia, España). Cuadernos Geología Ibérica 7:339–351

ASTM (2011) American Society for testing materials, annual book of ASTM standarts, Water and Environmental Technology, 11.01

Cánovas CR, Olías M, Nieto JM, Sarmiento AM, Cerón JC (2007) Hydrogeochemical characteristics of the Tinto and Odiel Rivers (SW Spain). Factors controlling metal contents. Sci Total Environ 373:363–382

Cidu R, Caboi R, Fanfani L, Frau F (1997) Acid drainage from sulfides hosting gold mineralization (Furtei, Sardinia). Env Geol 30:231–237

Ficklin WH, Plumlee GS, Smith KS, Mchugh JB (1992) Geochemical classification of mine drainages and natural drainages in mineralized areas. In: Kharaka Maest (ed) Water-rock interaction volume 1: low temperature environments. Balkema, Rotterdam, pp 381–384

Foster AL, Munk L, Koski RA, Shanks WC III, Stillings LL (2008) Relationships between microbial communities and environmental parameters at sites impacted by mining of volcanogenic massive sulfide deposits, Prince William Sound, Alaska. Appl Geochem 23(2):279–307

Gomes MEP, Favas PJC (2006) Mineralogical controls on mine drainage of the abandoned Ervodosa tin mine in north-eastern Portugal. Appl Geochem 21:1322–1334

Koski RA, Munk LA, Foster AL, Shanks WC III, Stillings LL (2008) Sulfide oxidation and distribution of metals near abandoned copper mines in coastal environments, Prince William Sound, Alaska, USA. Appl Geochem 23(2):227–254

Lehmann B (1990) Metallogeny of tin. Lecture notes in earth sciences. Springer, Berlin

Pereira ES (1987) Estudo geológico: estrutural da região de celorico de basto e sua interpretação geodinâmica. PhD Thesis, Faculdade de ciências da Universidade de Lisboa e Serviços Geológicos de Portugal, Lisboa

Pereira E (1989) Notícia explicativa da folha 10-A, celorico de basto. Serviços Geológicos de Portugal, Lisboa

Romero A, González I, Galán E (2010) Stream water geochemistry from mine wastes in Peña de Hierro, Riotinto area, SW Spain: a case of extreme acid mine drainage. Environ Earth Sci. doi: 10.1007/s12665-010-0554-y

Schmiermund RL, Drozd MA (1997) Acid mine drainage and other mining-influenced waters (MIW). In: Marcus J (ed) Mining environmental handbook: effects of mining on the environment and American environmental controls on mining. Imperial College Press, London, pp 599–617

Seal RR II, Shanks WC III (2008) Sulfide oxidation: insights from experimental, theoretical, stable isotope, and predictive studies in the field and laboratory. Appl Geochem 23(2):101–342

Silva EF, Bobos I, Matos JX, Patinha C, Reis AP, Fonseca EC (2009) Mineralogy and geochemistry of trace metals and REE in volcanic massive sulfide host rocks, stream sediments, stream waters and acid mine drainage from the Lousal mine area (Iberian Pyrite Belt, Portugal). Appl Geochem 24:383–401

USEPA (1991) Methods for measuring the acute toxicity of effluents and receiving waters to freshwater and marine organisms. In: Weber C (ed) Environmental monitoring systems laboratory. Cincinnati, Ohio: Office of Research and Development US. Environmental Protection Agency, Designation: EPA/600/4-89/001

Valente TM, Gomes CL (2009) Occurrence, properties and pollution potential of environmental minerals in acid mine drainage. Sci Total Environ 407:1135–1152